IOPscience iopscience.iop.org

Home Search Collections Journals About Contact us My IOPscience

First-principles investigation on the atomic structure and stability of a Pt monolayer on Fe(001)

This article has been downloaded from IOPscience. Please scroll down to see the full text article.

2007 J. Phys.: Condens. Matter 19 482002

(http://iopscience.iop.org/0953-8984/19/48/482002)

View the table of contents for this issue, or go to the journal homepage for more

Download details:
IP Address: 129.252.86.83
The article was downloaded on 29/05/2010 at 06:54

Please note that terms and conditions apply.

IOP FTC

IOP PUBLISHING JOURNAL OF PHYSICS: CONDENSED MATTER

J. Phys.: Condens. Matter **19** (2007) 482002 (7pp) doi:10.1088/0953-8984/19/48/482002

FAST TRACK COMMUNICATION

First-principles investigation on the atomic structure and stability of a Pt monolayer on Fe(001)

M C Escaño, H Nakanishi and H Kasai[1]

Department of Precision Science and Technology and Applied Physics, Osaka University, 2-1 Yamadaoka Suita, Osaka 565-0871, Japan

E-mail: kasai@dyn.ap.eng.osaka-u.ac.jp

Received 3 October 2007, in final form 29 October 2007
Published 13 November 2007
Online at stacks.iop.org/JPhysCM/19/482002

Abstract
We investigated the atomic structure and stability of a Pt monolayer on Fe(001) using spin-polarized density functional theory (DFT)-based total energy calculations. The results show that addition of a Pt monolayer on Fe substrate completely removes Fe(001) surface relaxation and induces minimal disordering of Fe atoms in the interior region in accordance with experimental findings. The stable distance between the Pt monolayer and the Fe substrate is 1.630 Å and the binding energy of Pt on Fe (per surface atom) is 2.00 eV. Comparison of such a binding energy with Pt–Pt binding in the first adjacent fcc Pt(001) layers shows that Pt binds more on Fe than with its corresponding pure metal slab. Such strong binding results in stabilization of the Pt monolayer on Fe(001) as verified by an increase in charge density within the Pt–Fe interface. Interestingly, addition of a Pt monolayer also induces enhancement of Fe–Fe interlayer binding in the interior region.

(Some figures in this article are in colour only in the electronic version)

1. Introduction

Polymer electrolyte fuel cells (PEFCs), with their high efficiency, low temperature operation, fuel flexibility and zero-emission, offer a promising alternative to conventional power generation systems for both stationary and mobile applications. However, commercialization of PEFCs involves economic obstacles, one of which is the high cost of platinum used to catalyze hydrogen oxidation in the anode and the oxidation reduction reaction (ORR) in the cathode. Recently, an overlayer structure of Pt on a non-noble metal was introduced as a potential alternative to pure Pt electrocatalyst, primarily because of its enhanced catalytic activity for the ORR and its ultra-low Pt content (about 90% reduction based on standard Pt loading) [1].

[1] Author to whom any correspondence should be addressed.

Other Pt alloy systems such as Pt_3M (M = 3d transition metal) have also been recognized in terms of their much improved catalytic activity for the ORR than pure Pt [2–5]. Since the Pt_3M type structures have a generally higher Pt content than the Pt overlayer structures on non-noble metals, the latter system has attracted considerable attention in cathode catalyst design. New processes for atomic layer deposition have already emerged, so nanofabrication of such systems is plausible. Taking advantage of the fact that one can take advantage of the metal–substrate interaction inherent in such bimetallic systems with considerably small lattice mismatch to tailor Pt catalytic property has paved the way for considering a Pt monolayer on Fe(001) {Pt_{ML}/Fe(001)}. Spin-resolved photoemission studies of Pt film on Fe(001) show Pt ferromagnetic coupling to Fe as a result of strong interaction between Fe 3d and Pt 5d states [6, 7]. Spin-polarized density functional theory (DFT) study of O_2 dissociative adsorption on Pt_{ML}/Fe(001) shows that the system demonstrates a favorable catalytic property as it produces a combination of a lower activation barrier for O_2 dissociation and weaker O binding than clean Pt(001) as a consequence of modification of Pt electronic surface structure by Fe [8]. Such properties are beneficial for the production of adsorbed O and for easier subsequent reactions such as the four-electron reduction of oxygen ($\frac{1}{2}O_2 + 2H^+ + 2e^- = H_2O$). With such promising catalytic properties of a Pt monolayer on Fe substrate the need for fundamental understanding of the structure's stability arises. There has been general agreement on the fact that stability is the foremost concern for potential catalyst applications. So far no *ab initio* calculations have focused on such stability arguments in the Pt–Fe bimetallic system. As a first step, therefore, in this current investigation we deal with the atomic structure and stability of a Pt monolayer on Fe(001). Herein, we show the optimized atomic structure with reference to clean Fe(001). Pt binding on Fe and its consequent effect on the Fe(001) surface is presented. Clearly, stability is a profound area of interest which requires understanding of other non-trivial issues such as the stability of the structure against adsorbates, water or an acid environment which may be considered for a more realistic simulation of fuel cell operating conditions. This study, however, presents the stability of the system with respect to reconstructions and surface relaxations which clarifies the system's structure, thus providing fundamental insights on which further rational cathode catalyst design may be based.

2. Computational details

We carried out spin-polarized DFT-based total energy calculations using the first-principles simulation code Vienna *ab initio* simulation package (VASP) [9–12]. Ionic cores are described by PAW potentials [13] and the Kohn–Sham one-electron valence states are expanded in the plane waves basis with a well-converged kinetic energy cutoff of 300 eV. The surface Brillouin zone integration is performed using the Monkhorst and Pack **k**-point sampling technique with $11 \times 11 \times 1$ sampling meshes. For the exchange correlation energy, the generalized gradient approximation (GGA) within the Perdew–Burke–Ernzerhof (PBE) functional [14, 15] was employed. The Fe substrate was simulated by a slab of seven bcc Fe(001) layers. The Pt_{ML}/Fe(001) system was modeled by a monolayer of Pt atoms pseudomorphically laid on top of the Fe(001) layers. Each supercell was constructed with ~10.00 Å of vacuum separating the slabs. Lateral and interlayer Fe–Fe distances for both systems are initially set based on the theoretically predicted equilibrium lattice constant which is 2.834 Å obtained by using an $11 \times 11 \times 11$ k-mesh on the primitive two-atom bcc unit cell for bulk Fe. Such a calculated lattice constant is in excellent agreement with previous DFT–PAW–GGA calculation [16] and with experimental results [17, 18]. The initial Pt distance from the first Fe layer of the bcc Fe(001) slab was set at 3.25 Å. Lateral and vertical atomic positions were relaxed except for the two bottom layers where the interlayer distance is fixed at the calculated bulk value,

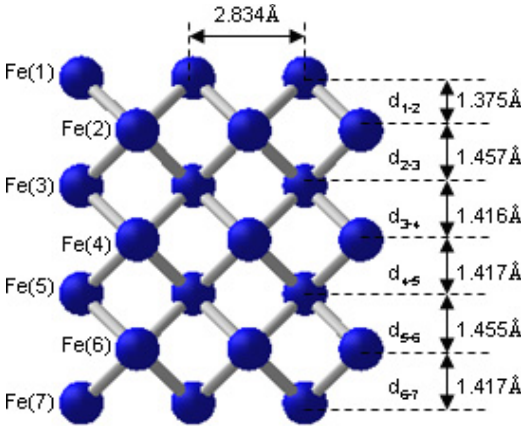

Figure 1. Optimized structure of Fe(001). d_{n1-n2} (where $n1$ and $n2$ are adjacent layers) represents the interlayer spacing. The values for corresponding interlayer distances are shown. Fe(n) shows an atom at a corresponding layer.

1.417 Å. By comparing the total energies of the two Pt_{ML}/Fe(001) configurations, that is, (a) Pt at $Z = 3.25$ Å from the Fe substrate and (b) Pt at an optimized distance from Fe substrate, we extract the binding energy (per surface atom) of Pt on Fe. This difference in total energy is interpreted as an indication of the stability of the Pt monolayer on Fe(001). The same process was employed to determine Pt–Pt binding in the first interlayer of a seven-layer slab of fcc Pt(001) as a suitable comparison. The charge density difference, which has been regarded in density functional theory as a key quantity for clarifying binding, was depicted more particularly within Pt–Fe and Fe–Fe interfaces.

3. Results and discussion

We first discuss the atomic structure of the reference system, Fe(001). The optimized structure is shown in figure 1 where d_{n1-n2} ($n1$ and $n2$ are corresponding adjacent layers) represents the interlayer spacing. The corresponding values are given. The trend in the changes in the interlayer distances expressed as a percentage change with respect to the bulk value ($\Delta d_{n1-n2}/d_{\text{bulk}}$) is consistent with experimental results [18, 19]. Table 1 gives the values of such percentage changes with corresponding experimentally derived percentage ranges (in brackets) based on low-energy electron diffraction (LEED) study in [18]. We note a significant contraction (3.0%) in the first interlayer indicative of a downward Fe(001) surface relaxation. Moreover, the succeeding interlayer and the d_{5-6} interlayer both exhibit significant expansion, while interlayer spacings, d_{3-4}, d_{4-5}, remain almost unchanged. The local magnetic moment in μ_B per Fe atom denoted by Fe(n), where n corresponds to a layer of Fe(001) (see figure 1), is shown in the third column of table 1. The Fe(4) magnetic moment represents the magnetic moment for bulk Fe, which agrees well with the predicted local magnetic moment in [16] and with the experimentally derived value [20, 21]. It is equally important to note the significant difference in the local magnetic moments of Fe(1) and Fe(7) which are thought to have resulted from the difference in the geometries of the two surfaces, represented by opposite sides of the slab, due to Fe surface relaxation.

For the Pt_{ML}/Fe(001) system, figure 2 gives the optimized structure. The same notations are used for the interlayer distances as for Fe(001). The corresponding values for interlayer

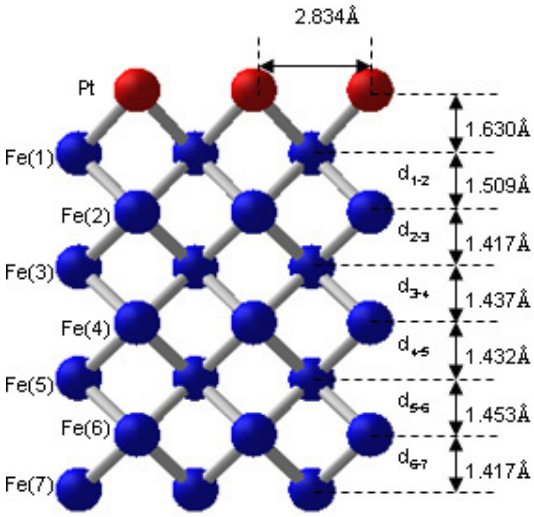

Figure 2. Optimized structure of Pt_{ML}/Fe(001). d_{n1-n2} (where $n1$ and $n2$ are adjacent layers) represents the corresponding interlayer spacing. The optimized Pt layer distance from Fe is 1.630 Å. The values for the corresponding interlayer distances are shown. Fe(n) shows an atom at a corresponding layer.

Table 1. Change in the interlayer distances in Fe(001) expressed as a percentage change with respect to the bulk value and the local magnetic moments in μ_B per Fe atom specified by Fe(n) where n is the corresponding layer as shown in figure 1. {*} indicates no reported measurement.

d_{n1-n2}	$\Delta d_{n1-n2}/d_{bulk}$ (%) {Expt}	Local magnetic moment (μ_B)
d_{1-2}	−3.0{−7.0 − (−2.0)}	2.96 {Fe(1)}
d_{2-3}	+2.8{−0.7 − 5.3}	2.33 {Fe(2)}
d_{3-4}	−0.1{−3.5 − 2.5}	2.43 {Fe(3)}
d_{4-5}	0.0{*}	2.26 {Fe(4)}
d_{5-6}	+2.7{*}	2.43 {Fe(5)}
d_{6-7}	Fixed at bulk value	2.38 {Fe(6)}
		2.98 {Fe(7)}

spacings are shown. Table 2 gives the percentage change in interlayer distances with respect to the corresponding interlayer in optimized Fe(001) which we denote as $d_{n1-n2(Fe)}$. Interestingly, the surface relaxation of Fe(001) was completely removed upon addition of a Pt monolayer. In fact, there is a significant expansion of the first interlayer distance (d_{1-2}) which indicates a strong Pt–Fe binding. No lateral reconstruction was observed in Fe(001) upon addition of a Pt monolayer. The lateral Pt–Pt distance adopts the Fe lattice constant in conformity with LEED studies showing epitaxial growth of thin Pt film on Fe(001) [7, 17, 18]. We note minimal changes in the atomic positions of Fe in d_{3-4} to d_{5-6} which suggests that Pt indeed does not induce significant disordering of Fe atoms underneath [18]. The calculated induced Pt magnetic moment is 0.42 μ_B in accordance with the experimentally determined value of ∼0.50 μ_B for Pt atom on (001)Fe/Pt multilayers using x-ray magnetic circular dichroism (XMCD) [20]. The calculated local magnetic moment in μ_B per Fe atom denoted by Fe(n), is shown in the third column of table 2. The magnetic moment of an Fe atom in the first layer is somehow quenched upon binding to Pt, which may indicate strong Pt–Fe interaction.

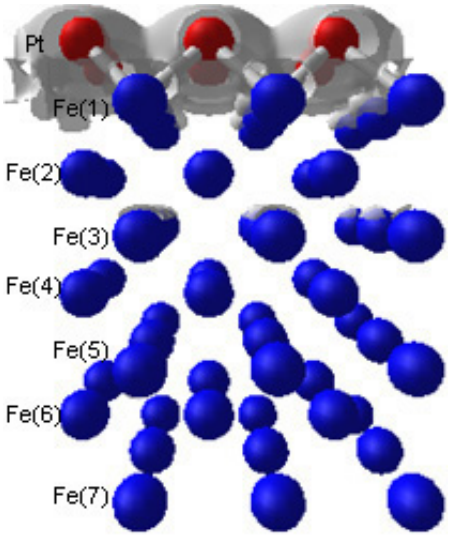

Figure 3. Charge density difference (positive) distribution at an isosurface value of 0.200 eV Å^{-3} for Pt_{ML}/Fe(001), showing increased charge distribution within the Pt–Fe interface, more specifically near Pt atom sites, and bonds indicating strong Pt–Fe binding. Depletion of charge density is observed in Fe–Fe interfaces.

Table 2. Pt_{ML}/Fe(001) change in the interlayer distances expressed as a percentage change with respect to the corresponding interlayer distance in optimized Fe(001): $\Delta d_{n1-n2}/d_{n1-n2(\mathrm{Fe})}(\%)$ and the local magnetic moments in μ_B are shown per Fe atom specified by Fe(n) where n is the corresponding layer as shown in figure 2.

d_{n1-n2}	$\Delta d_{n1-n2}/d_{n1-n2(\mathrm{Fe})}$ (%)	Local magnetic moment (μ_B)
d_{1-2}	+9.8	2.90 {Fe(1)}
d_{2-3}	−2.8	2.55 {Fe(2)}
d_{3-4}	+1.5	2.34 {Fe(3)}
d_{4-5}	+1.1	2.39 {Fe(4)}
d_{5-6}	−1.4	2.44 {Fe(5)}
d_{6-7}	Fixed at bulk value	2.40 {Fe(6)}
		2.98 {Fe(7)}

To determine the stability of a Pt monolayer on Fe substrate, we calculated the binding energy (per surface atom) of Pt on Fe at the optimized Pt monolayer distance from Fe(001), which is 1.630 Å. We found that Pt binds more with Fe substrate (2.00 eV) than with its corresponding pure metal slab (1.50 eV). The Pt–Fe bond length is also significantly contracted by 7.2% with respect to the Pt–Pt bond length in Pt(001). This conforms to the strong metal–metal interlayer binding in such bimetallic systems [22, 23].

For the sake of further verification of the strong Pt–Fe binding we plot the charge density difference distribution for Pt_{ML}/Fe(001) taken by subtracting the charge density of the Pt_{ML}/Fe(001) configuration (a) from (b) described previously. Figure 3 displays the positive difference between such densities with an isosurface value of 0.200 eV Å^{-3}. We note an accumulation of charge densities in the region between Pt and Fe, more specifically near the Pt atom sites and bonds. Such an increase in charge density around this region supports strong Pt–Fe binding. Depletion of charge density is observed within Fe–Fe interfaces. However, at

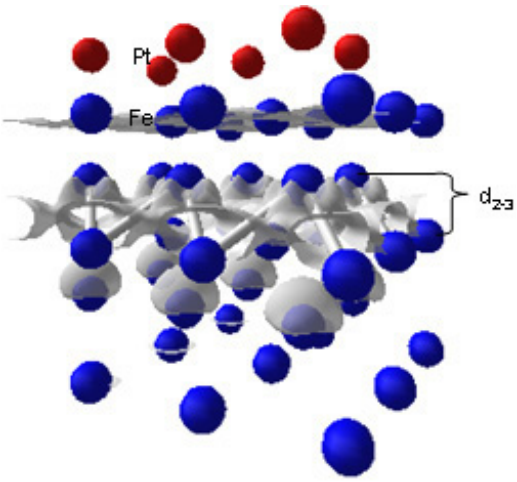

Figure 4. Charge density difference (positive) distribution at an isosurface value of 0.085 eV Å^{-3} for Pt_{ML}/Fe(001), showing increased charge distribution within d_{2-3} interlayer indicating enhancement of Fe–Fe binding in this region.

some isosurface value of 0.085 eV Å^{-3}, a region of increased charge density near atom sites and along the bonds formed by Fe atoms in the second layer with those in the third layer emanates as shown in figure 4. This suggests enhancement of d_{2-3} interlayer binding upon addition of a Pt monolayer. The previously noted contraction in such an interlayer with respect to the reference system, Fe(001), may explain such enhancement. Surprisingly, addition of a Pt monolayer seems to further enhance Fe–Fe binding in the mid-interior region.

4. Conclusion

We performed spin-polarized DFT-based total energy calculations to investigate the atomic structure and stability of a Pt monolayer on Fe(001). The calculations results show that addition of a Pt monolayer completely removes Fe(001) surface relaxation. The stable distance between Pt and the Fe substrate is 1.630 Å. Pt binding on Fe is observed to be stronger than on its corresponding pure metal slab. Such stabilization of a Pt monolayer on Fe(001) is verified by an accumulation of charge density within the Pt–Fe interface. Increase in charge density is also observed within the second Fe–Fe interlayer, consistent with the contraction of such an interlayer upon Pt layer binding on Fe.

Acknowledgments

This work is supported by the Ministry of Education, Culture, Sports, Science and Technology of Japan (MEXT) through their Grants-in-Aid for Scientific Research on Priority Areas (Developing Next Generation Quantum Simulators and Quantum-Based Design Techniques), Special Coordination Funds for the 21st Century Center of Excellence (COE) program (G18) 'Core Research and Advance Education Center for Materials Science and Nano-Engineering', Grants-in-Aid for Scientific Research supported by the Japan Society for the Promotion of Science (JSPS) and the 'Research and Development of Polymer Electrolyte Fuel Cell Systems' project of the New Energy and Industrial Technology Development Organisation (NEDO). Some of the calculations were done using computer facilities of the ISSP Super Computer

Center (University of Tokyo), the Yukawa Institute (Kyoto University) and the Japan Atomic Energy Agency (ITBL, JAEA).

References

[1] Sasaki K, Zhang J, Wang J, Uribe F and Adzic R 2006 *Res. Chem. Intermed.* **32** 543–59
[2] Toda T, Igarashi H and Watanabe M 1998 *J. Electrochem. Soc.* **145** 4185
[3] Jalan V and Taylor E J 1983 *J. Electrochem. Soc.* **130** 2299
[4] Mukurjee S, Srinivasan S, Soriaga M P and McBreen J 1995 *J. Electrochem. Soc.* **142** 1409
[5] Toda T, Igarashi H, Uchida H and Watanabe M 1999 *J. Electrochem. Soc.* **146** 3750
[6] Finazzi M and Braicovich L 1995 *Phys. Rev.* B **50** 14671
[7] Bertacco R and Ciccacci F 1997 *Phys. Rev.* B **57** 96
[8] Escano C, Kishi T, Kunikata S, Nakanishi H and Kasai H 2007 *J. Surf. Sci. Nanotechnol.* **5** 117–20
[9] Kresse G and Furthmüller J 1996 *Comput. Mater. Sci.* **6** 15
[10] Kresse G and Furthmüller J 1996 *Phys. Rev.* B **54** 11169
[11] Kresse G and Hafner J 1993 *Phys. Rev.* B **47** 558
[12] Kresse G and Hafner J 1994 *Phys. Rev.* B **49** 14251
[13] Blöchl P E 1994 *Phys. Rev.* B **50** 17953
[14] Perdew J P, Burke K and Ernzerhof M 1996 *Phys. Rev. Lett.* **77** 3865
[15] Perdew J P, Burke K and Ernzerhof M 1997 *Phys. Rev. Lett.* **78** 1396
[16] Johnson D F, Jiang D E and Carter E A 2007 *Surf. Sci.* **601** 699
[17] Hufnagel T C, Kautzky M C, Daniels B J and Clemens B M 1999 *J. Appl. Phys.* **85** 5
[18] Leibbrandt G W R, Van Wijk R and Habraken F H P M 1992 *Phys. Rev.* B **47** 6630
[19] Wang Q, Li Y S, Jona F and Marcus P M 1987 *Solid State Commun.* **61** 623
[20] Lyubina J, Opahle I, Richter M, Gutfleisch O, Müller K and Schultz L 2006 *Appl. Phys. Lett.* **89** 032505
[21] Antel W J Jr, Schiwickert M M, Lin T, O'Brien W L and Harp G R 1999 *Phys. Rev.* B **60** 12933
[22] Rodriguez J A and Goodman D W 1992 *Science* **257** 897–903
[23] Wu R and Freeman A J 1995 *Phys. Rev.* B **52** 16